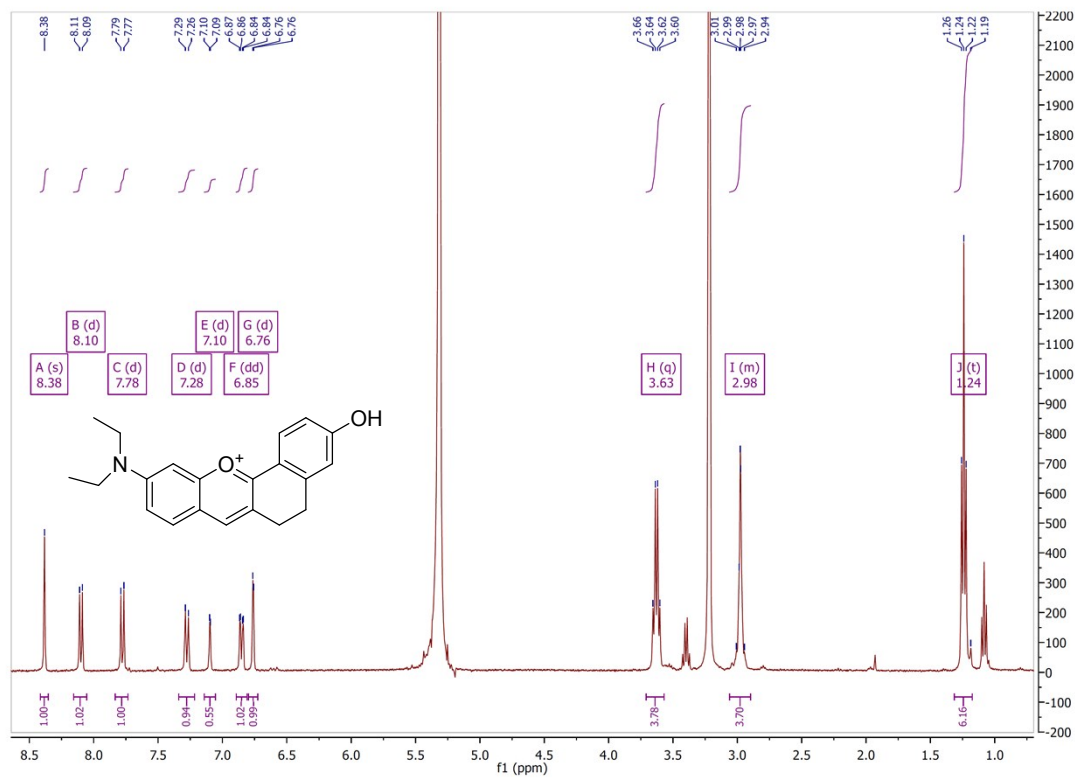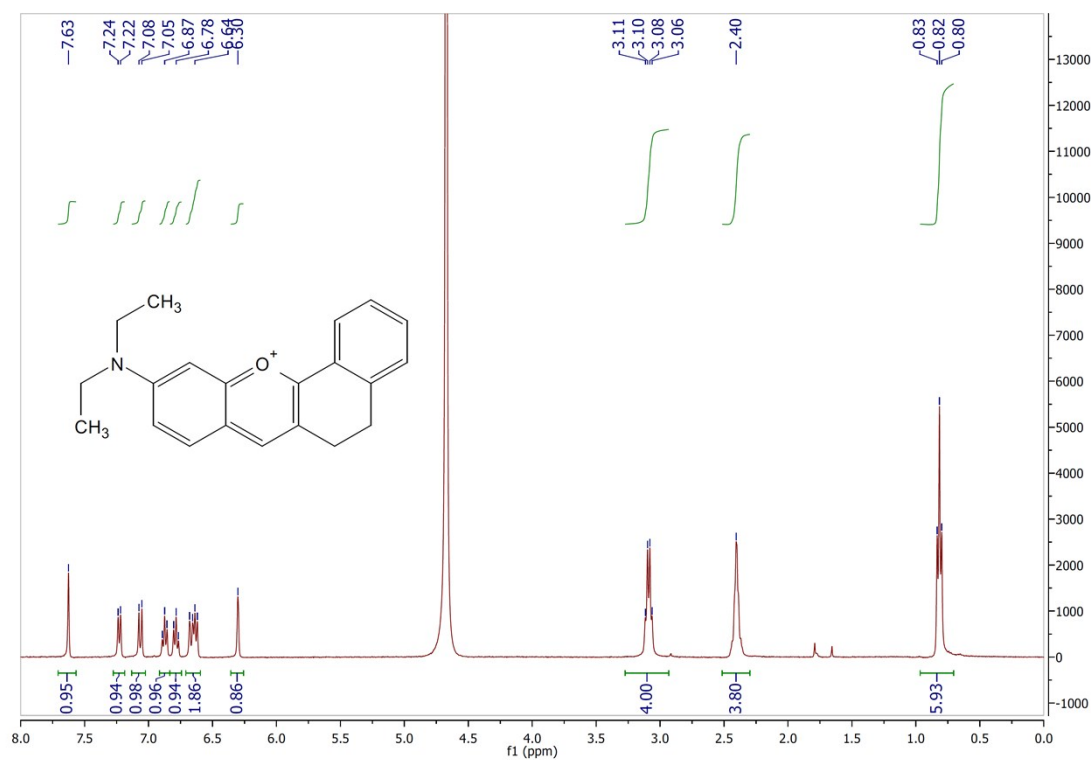**Exploring the 7-Diethylaminoflavylium Derivatives Multistate of Chemical Reactions in the presence of CTAB micelles. Thermodynamic Reversibility Achieved Through Different Kinetic Pathways.**

Márcia Pessêgo [a)], Nuno Basílio, [a)]* Johan Mendoza [a)], João Avó [a)], Luís Cunha-Silva [b)], A. Jorge Parola and Fernando Pina [a)]*

¹H NMR

Figure S1A – ¹H NMR spectrum of compound 1 in D_2O with DCl ≈ 0.1 M.

Figure S2A – ¹H NMR spectrum of compound 1 in CD_3OD with DCl ≈ 0.1 M.

Structural Data

Table S1. Crystal and structure refinement data for compounds **1**·BF$_4$, **2**·HSO$_4$_M and **2**·HSO$_4$_O.

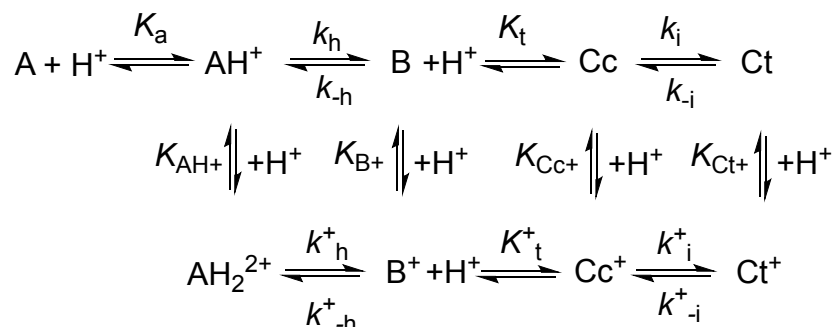|	**1**·BF$_4$	**2**·HSO$_4$_M	**2**·HSO$_4$_O
Chemical formula	C$_{21}$H$_{22}$BF$_4$NO	C$_{21}$H$_{23}$NO$_6$S	C$_{21}$H$_{23}$NO$_6$S
M$_r$	391.20	417.46	417.46
Crystal description	Brown prism	Brown block	Brown needle
Crystal size /mm	0.20 × 0.12 × 0.10	0.35 × 0.17 × 0.07	0.15 × 0.02 × 0.01
Crystal system, space group	Monoclinic, *C*2/c	Monoclinic, *P*2$_1$/*c*	Orthorhombic, *Pna*2$_1$
a /Å	17.6076(16)	11.3956(7)	19.606(9)
b /Å	17.9505(12)	14.0481(9)	11.969(5)
c /Å	14.4826(13)	13.0280(8)	8.053(4)
α /°	90	90	90
β /°	125.893(3)	114.240(3)	90
γ /°	90	90	90
Volume /Å^3	3708.2(5)	1901.7(2)	1889.7(2)
Z	8	4	4
ρ$_{calculated}$ /g cm^{-3}	1.401	1.458	1.467
F(000)	1632	880	880
μ /mm^{-1}	0.112	0.211	0.212
θ range /°	3.649 to 26.372	3.724 to 25.678	3.690 to 25.018
Index ranges	$-20 \leq h \leq 22$ $-22 \leq k \leq 22$ $-18 \leq l \leq 18$	$-13 \leq h \leq 13$ $-17 \leq k \leq 17$ $-15 \leq l \leq 15$	$-23 \leq h \leq 23$ $-14 \leq k \leq 14$ $-9 \leq l \leq 9$
Reflections collected	19043	50030	16423
Independent reflections	3784 (R_{int} = 0.0462)	3570 (R_{int} = 0.0348)	3089 (R_{int} = 0.1918)
Final *R* indices [F^2>2σ(F^2)]	R_1 = 0.0495 wR_2 = 0.1112	R_1 = 0.0334 wR_2 = 0.0870	R_1 = 0.0644 wR_2 = 0.0995
Final *R* indices (F^2)	R_1 = 0.0831 wR_2 = 0.1277	R_1 = 0.0422 wR_2 = 0.0931	R_1 = 0.1196 wR_2 = 0.1450
Δρ$_{max}$ and Δρ$_{min}$ /e.Å^{-3}	0.351 and -0.389	0.243 and -0.437	0.421 and -0.307
CCDC numbers	1543226	1543228	1543227

Table S2. Geometric information (distances in Å and angles in degrees) of the D–H···A hydrogen bond interactions present in the structures of **1**·BF$_4$, **2**·HSO$_4$_M and **2**·HSO$_4$_O.[a]

	D–H···A	d(H···A)	d(D···A)	∠(DHA)
1·BF$_4$	C2−H2A···F2[ii]	2.51	3.459(3)	159.9
	C3−H3A···F1[i]	2.60	3.576(3)	169.0
	C3−H3B··· F2[ii]	2.55	3.506(3)	163.4
	C6−H6···F4[iii]	2.41	3.315(3)	158.4
2·HSO$_4$_M	O1−H1···O3	1.81(1)	2.731(2)	172(2)
	O4−H4···O5[iv]	1.71(1)	2.642(2)	175(2)
	C3−H3···O5[v]	2.57	3.435(2)	150.7
	C7−H7···O3[vi]	2.46	3.436(2)	167.4
	C16−H16···O1[vii]	2.42	3.237(2)	143.9
	C17−H17···O3[vii]	2.50	3.429(3)	165.2
	C18−H18···O4[iii]	2.67	3.496(3)	140.8
2·HSO$_4$_O	O1−H1···O3	1.71(2)	2.652(8)	175(7)
	O4−H4···O5[viii]	1.64(2)	2.582(7)	172(8)
	C6−H6···O3	2.66	3.310(10)	126.5
	C14−H14···O6[iii]	2.40	3.340(10)	167.9
	C16−H16···O1[ix]	2.38	3.272(10)	156.8
	C19−H19C···O2[iii]	2.62	3.433(9)	140.9

[a] Symmetry transformations used to generate equivalent atoms:
(i) −x, y, −z+3/2; (ii) x+1/2, −y−1/2, z+1/2; (iii) x, y, z+1;
(iv) 1−x, −y+1, −z−1; (v) −x, −y+1, −z; (vi) x+1/2, −y+3/2, z+1/2;
(vii) x+1, y, z+1; (vii) x+1, y, z+1; (viii) −x+1, −y+1, z+1/2; (ix) −x+3/2, y+1/2, z+3/2.

Mathematical treatment

$$A + H^+ \overset{K_a}{\rightleftharpoons} AH^+ \underset{k_{-h}}{\overset{k_h}{\rightleftharpoons}} B + H^+ \overset{K_t}{\rightleftharpoons} Cc \underset{k_{-i}}{\overset{k_i}{\rightleftharpoons}} Ct$$

$$K_{AH+} \updownarrow +H^+ \quad K_{B+} \updownarrow +H^+ \quad K_{Cc+} \updownarrow +H^+ \quad K_{Ct+} \updownarrow +H^+$$

$$AH_2^{2+} \underset{k^+_{-h}}{\overset{k^+_h}{\rightleftharpoons}} B^+ + H^+ \overset{K^+_t}{\rightleftharpoons} Cc^+ \underset{k^+_{-i}}{\overset{k^+_i}{\rightleftharpoons}} Ct^+$$

Scheme S1. Aminoflavylium network of chemical reactions in acidic conditions.

In order to deduce the expression that accounts for the kinetics of the network shown in Scheme A1 the following assumption are made:

1- All proton transfer reactions are much faster than the hydration, tautomerization and isomerization reactions.

2- The tautomerization is assumed to be faster than the hydration and isomerization. Thus, B and Cc; and, as well B^+ and Cc^+ are assumed to be in equilibrium during the interconversion kinetics to reach the equilibrium after a pH jump.

3- B+Cc and B^++Cc^+ are steady state transient species.

Before the hydration start to take place the total concentration of flavylium cation is given by:

$$[AH^+]_t = [AH^+] + [A] + [AH_2^{2+}] \tag{S1}$$

Because $[AH_2^{2+}]$ is only formed in extremely acidic conditions this species can be discarded. Thus, the pH-dependent equilibrium concentration of $[AH^+]$ is given by:

$$[AH^+] = \left(\frac{[AH^+]_t [H^+]}{[H^+] + K_a} \right) \tag{S2}$$

Assuming a fast equilibrium between the Cc and B species the following expressions account for the concentrations of these species:

$$[B + Cc]_t = [B] + [Cc] + [B^+] + [Cc^+] \qquad (S3)$$

$$K_t = \frac{[Cc]}{[B]} \qquad (S4)$$

$$K_{B+} = \frac{[B][H^+]}{[B^+]} \qquad (S5)$$

$$K_{Cc+} = \frac{[Cc][H^+]}{[Cc^+]} \qquad (S6)$$

After some algebraic manipulations:

$$[B] = \frac{K_{B+}K_{Cc+}}{K_{B+}K_{Cc+} + K_tK_{B+}K_{Cc+} + K_{Cc+}[H^+] + K_tK_{B+}[H^+]}[B + Cc]_t \qquad (S7)$$

$$[Cc] = \frac{K_tK_{B+}K_{Cc+}}{K_{B+}K_{Cc+} + K_tK_{B+}K_{Cc+} + K_{Cc+}[H^+] + K_tK_{B+}[H^+]}[B + Cc]_t \qquad (S8)$$

$$[B^+] = \frac{K_{Cc+}[H^+]}{K_{B+}K_{Cc+} + K_tK_{B+}K_{Cc+} + K_{Cc+}[H^+] + K_tK_{B+}[H^+]}[B + Cc]_t \qquad (S9)$$

$$[Cc^+] = \frac{K_tK_{B+}[H^+]}{K_{B+}K_{Cc+} + K_tK_{B+}K_{Cc+} + K_{Cc+}[H^+] + K_tK_{B+}[H^+]}[B + Cc]_t \qquad (S10)$$

The rate for the formation and consumption of B and Cc from the hydration and isomerization reactions is given by:

$$\frac{d[B + Cc]_t}{dt} = k_h[AH^+] - k_{-h}[B][H^+] - k_i[Cc] + k_{-i}[Ct] \qquad (S11)$$

The protonation of the trans-chalcone must be accounted by equation S12:

$$[Ct] = \frac{[Ct]_t K_{Ct+}}{\left(K_{Ct+} + [H^+]\right)} \qquad (S12)$$

Combining equations S2, S7, S8 and S12 with the kinetic equation S11 leads to:

$$\frac{d[B+Cc]_t}{dt}$$

$$= \frac{[AH^+]_t [H^+]}{[H^+] + K_a} k_h - \frac{K_{B+} K_{Cc+} [H^+][B+Cc]_t}{K_{B+} K_{Cc+} + K_t K_{B+} K_{Cc+} + K_{Cc+} [H^+] + K_t K_{B+} [H^+]} k$$

$$k_i + \frac{K_{Ct+} [Ct]_t}{\left(K_{Ct+} + [H^+]\right)} k_{-i} \qquad (S13)$$

Assuming a steady-state for B+Cc:

$$[B+Cc]_t$$

$$= \left(\frac{[AH^+]_t [H^+]}{[H^+] + K_a} k_h + \frac{K_{Ct+} [Ct]_t}{\left(K_{Ct+} + [H^+]\right)} k_{-i}\right) \frac{K_{B+} K_{Cc+} + K_t K_{B+} K_{Cc+} + K_{Cc+} [}{K_{B+} K_{Cc+} [H^+] k_{-h} + K_t K}$$

$$(S14)$$

The rate of the flavylium consumption is given by:

$$-\frac{d[AH^+]_t}{dt} = k_h [AH^+] - k_{-h}[B][H^+] \qquad (S15)$$

Thus, after some algebraic manipulation, equation S17 can be obtained by considering an direct interconversion equilibrium between AH$^+$ and Ct (equation S16). It is worth noting that, experimentally, Ct forms at the same rate that AH$^+$ disappears.

$$-\frac{d[AH^+]_t}{dt}$$

$$= \left\{ k_h \left(\frac{[H^+]}{[H^+] + K_a} \right) - k_{-h} \left(\frac{K_{B+} K_{Cc+} [H^+]}{K_{B+} K_{Cc+} [H^+] k_{-h} + K_t K_{B+} K_{Cc+} k_i} \right) \left(\frac{[H^+]}{[H^+] + K_a} k \right.$$

$$\left. k_{-h} \left(\frac{K_{B+} K_{Cc+} [H^+]}{K_{B+} K_{Cc+} [H^+] k_{-h} + K_t K_{B+} K_{Cc+} k_i} \right) \left(\frac{K_{Ct+}}{\left(K_{Ct+} + [H^+]\right)} k_{-i} \right) [Ct]_t \right. \qquad (S16$$

$$k_{obs1}$$

$$= k_h\left(\frac{[H^+]}{[H^+]+K_a}\right) - k_{-h}\left(\frac{K_{B+}K_{Cc+}[H^+]}{K_{B+}K_{Cc+}[H^+]k_{-h}+K_tK_{B+}K_{Cc+}k_i}\right)\left(\frac{[H^+]}{[H^+]+K_a}\right)k$$

$$\left(\frac{K_{Ct+}}{(K_{Ct+}+[H^+])}k_{-i}\right) \qquad (S17)$$

$$k_{obs1} = \frac{\dfrac{[H^+]}{[H^+]+K_a}K_tK_hk_i + \dfrac{K_{Ct+}[H^+]}{K_{Ct+}+[H^+]}k_{-i}}{[H^+]+\dfrac{K_tk_i}{k_{-h}}} \qquad (S18)$$

Equation S18 holds for reaction channel corresponding to the unprotonated species. However, the overall reaction rate is given by the sum of this reaction channel with the one corresponding to the protonated species. The corresponding equation (S19) is readily obtained as above:

$$k_{obs2} = \frac{\dfrac{K_{AH+}K_h^+K_tK_{B+}[H^+]^2}{K_a+[H^+]+K_{AH+}[H^+]^2}k_i^+ + \dfrac{K_{Cc+}[H^+]^2}{K_{Ct+}+[H^+]}k_{-i}^+}{K_{Cc+}[H^+]+\dfrac{k_i^+K_tK_{B+}}{k_{-h}^+}} \qquad (S19)$$

$$k_{obs\,global} = k_{obs1} + k_{obs2}$$

$$= \frac{\dfrac{[H^+]}{[H^+]+K_a}K_tK_hk_i + \dfrac{K_{Ct+}[H^+]}{K_{Ct+}+[H^+]}k_{-i}}{[H^+]+\dfrac{K_tk_i}{k_{-h}}} + \frac{\dfrac{[H^+]^2}{K_a+[H^+]+K_{AH+}[H^+]^2}K_{AH+}K}{[H^+]+\dfrac{K}{}}$$

$$(S20)$$

Because the formation of $\left[AH_2^{2+}\right]$ is not observed under the experimental conditions:

$$k_{obs\,global} = \frac{\dfrac{[H^+]}{[H^+]+K_a}K_tK_hk_i + \dfrac{K_{Ct+}[H^+]}{K_{Ct+}+[H^+]}k_{-i}}{[H^+]+\dfrac{K_tk_i}{k_{-h}}} + \frac{\dfrac{[H^+]^2}{K_{Ct+}+[H^+]}k_{-i}^+}{[H^+]+\dfrac{K_t+k_i^+}{k_{-h}^+}} \qquad (S21)$$

In practice, the direct hydration of AH_2^{2+} is not observed because at very acidic pH values the flavylium cation is the stable species. On the other hand, under these conditions the dehydration is very fast and the *trans-cis* isomerization is rate limiting for reverse pH jumps from basic, neutral or slightly acidic to low pH values. Owing to these arguments, Equation S21 can be further simplified to S22:

$$k_{obs\ global} = \frac{\dfrac{[H^+]}{[H^+] + K_a}K_t K_h k_i + \dfrac{K_{Ct+}[H^+]}{K_{Ct+} + [H^+]}k_{-i}}{[H^+] + \dfrac{K_t k_i}{k_{-h}}} + \frac{[H^+]}{K_{Ct+} + [H^+]}k_{-i}^+ \quad (S22)$$

Characterization of compound 2

The introduction of a hydroxyl substituent in position 4' allows the formation of the quinoidal base, as shown in Fig. S1B(a), where the raising of this species at the expenses of the flavylium cation is observed. The obtained acidity constant is pK_a=6.0. The system at the equilibrium is shown in Fig.S1B(b). the multistate behaves as a single acid base equilibrium with acidity constant, pK'_a=3.8.

(a)   **(b)**
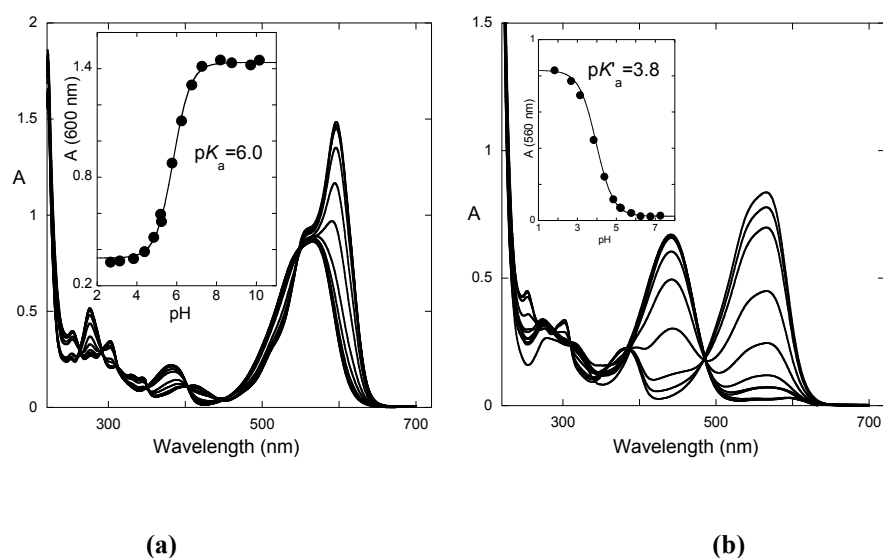
Figure S1B. (a) pH dependent spectral variations of compound 2 (2×10^{-5} M) in the presence of 0.020 M CTAB immediately after a direct pH jump; (b) the same at the equilibrium.

A series of direct and reverse pH jumps was carried out to define the bell shaped curve, Fig. S2B.

(a)   **(b)**
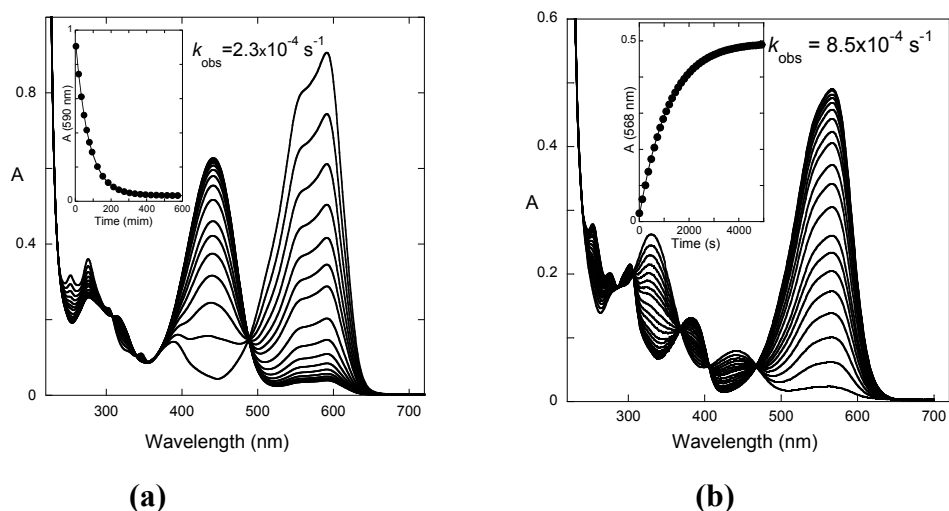
Figure S2B. (a) Spectral variations observed for compound 2 (2×10^{-5} M) in the presence of CTAB 0.020 M after a direct pH jump from pH=1 to 5.8; (b) the same for a reverse pH jump from equilibrated solutions at pH=10 (ionized *trans*-chalcone) to 0.7.

S10

Immediately after the direct pH jump the absorption of a mixture of flavylium cation and quinoidal base is observed. This absorption decreases to give the final absorption of the *trans*-chalcone, Fig. S2B(a). In the case of the reverse pH jumps the stock solution at pH=7 constituted by the *trans*-chalcone was used. Immediately after the pH jump and before observation of any flavylium cation formation, the chalcone protonates at the amine substituent giving the species Ct^+. The observed kinetic process corresponds to the disappearance of this last species to give the flavylium cation, Fig. S2B(b). Representation of the initial absorption spectra of the reversed pH jumps is shown in Fig. S3B, permitting to obtain the protonation constant of the amine substituent in the *trans*-chalcone $pK_{Ct+/Ct}=1.1$.
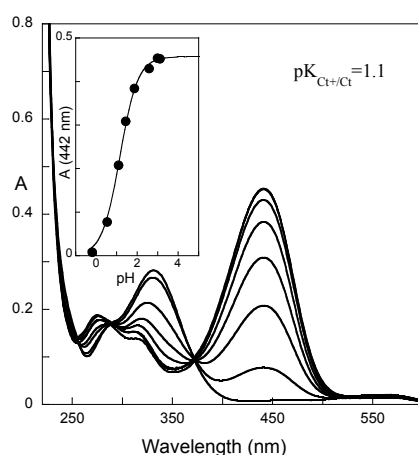
Figure S3B. Spectral variations of compound 2 (1.7×10^{-5} M) in the presence of 0.020 M CTAB micelles taken immediately after a reverse pH jump from equilibrated solutions of the *trans*-chalcone to acidic pH values.

Representation of the slower rate constants of the multistate by carrying out direct and reverse pH jumps 5 (as in Fig.S3B) at different final pH values is shown in Fig.S4B. Fitting was achieved with eq.(11) for the following parameters $K_h K_t k_i = 2.0 \times 10^{-8}$ Ms^{-1}; $K_t k_i / k_{-h} = 7.0 \times 10^{-5}$ M; $k_{-i} = 6 \times 10^{-5}$ s^{-1}; $pK_{Ct+/Ct} = 1.1$; $k_{-i+} = 1.5 \times 10^{-3}$ s^{-1}. We cannot exclude a contribution from the catalysis of the *cis-trans* isomerization under the stronger effect Ct^+ to give AH^+.
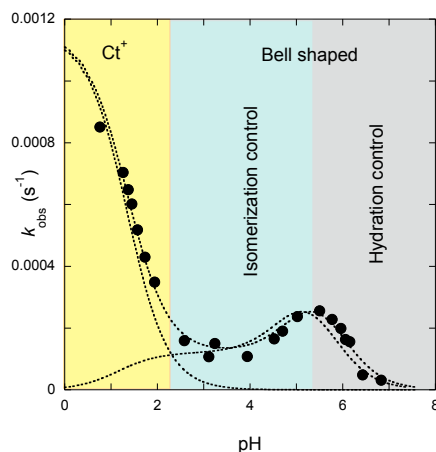
Figure S4B. Representation of the rate constants of the slower process of the interconversion kinetics for compound 2 in the presence of CTAB 0.020 M, versus pH. Fitting was achieved with eq.(11) for the following parameters: $K_h K_t k_i = 2 \times 10^{-8}$ Ms^{-1}; $K_t k_i / k_{-h} = 7.0 \times 10^{-5}$ M; $k_{-i} = 6 \times 10^{-5}$ s^{-1}; p$K_{Ct+/Ct} = 1.1$; $k_{-i+} = 1.5 \times 10^{-3}$ s^{-1}, $k_h = 2.9 \times 10^{-4}$ s^{-1}.

The flash photolysis of compound 2 in the presence of CTAB was also performed, Fig. S5B.
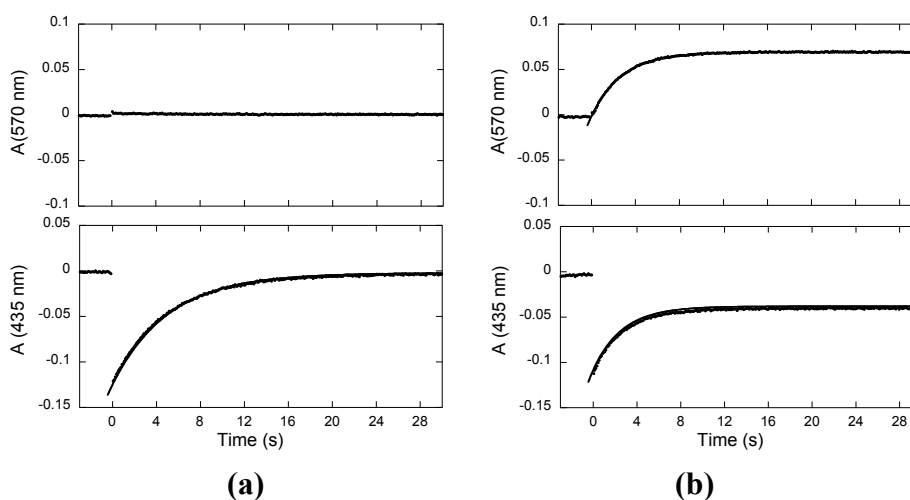
Figure S5B. Flash photolysis traces of the compound 2 in the presence of CTAB 0.020 M; **(a)** pH 7.3; $k_{obs} = 0.2$ s^{-1}; **(b)** pH=4.85 $k_{obs} = 0.36$ s^{-1}

After formation of *cis*-chalcone upon the flash two parallel and competitive reactions may occur: i) forward to give flavylium cation; ii) backward to restore *trans*-chalcone. Considering that the tautomerization reactions is much faster than hydration and isomerization[i] it is reliable to consider that the equilibrium between B and Cc is established at first and eq.(12) (see manuscript) accounts for the global flash photolysis

process. Fitting of eq.(12) (see manuscript) is achieved for $K_t/(1+K_t)k_i$=0.2 s^{-1} and $k_{-h}(1+K_t)$=2860 M^{-1}s^{-1}, Fig. S6B. In the same figure the yield of Ct recovery is reported, the respective fitting carried out with eq.(13) of the manuscript and the parameters used for fit eq.(11). The influence of the amine substituent protonation takes place for pH<4 and similar to compound 1 increases the yield of the Ct recovered when compared with the non protonated form.
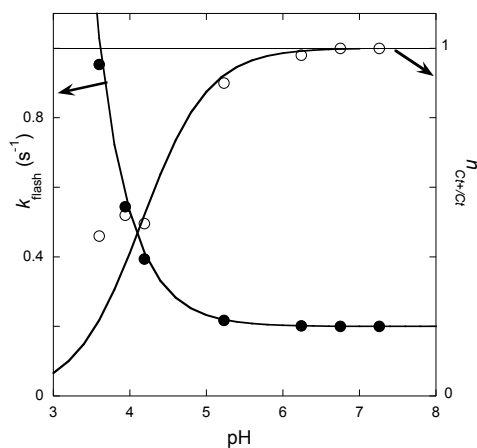

Figure S6B. Representation of the flash photolysis rate constants of the compound 2 in the presence of CTAB 0.020 M as a function of pH. Fitting was achieved with eq.(10) the rate and equilibrium constants previously calculated, Table 1, $k_i K_t/(1+K_t)$=0.2s^{-1}; k_{-h}/= $k_{-h}/(1+K_t)$ 2860 Ms^{-1}; yield of *trans*-chalcone recovery.

Characterization of compound 3

The absorption spectra taken immediately after direct pH jumps and at the equilibrium is shown in Fig. S1C(a) and b respectively pKa=6.2 pK'a=1.6
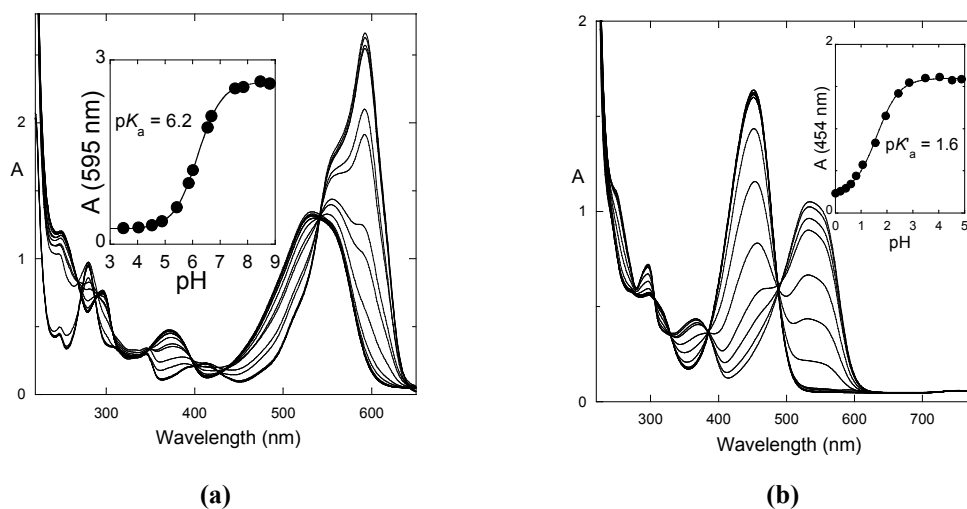

(a)   **(b)**

Figure S1C. (a) pH dependent spectral variations of compound 3 (3.8×10^{-5} M) in the presence of 0.020 M CTAB immediately after a direct pH jump; (b) the same at the equilibrium.
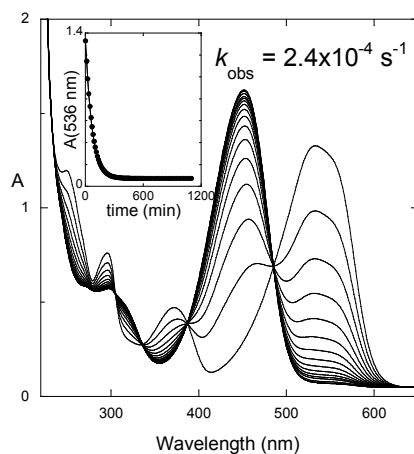

Figure S2C. Spectral variations of compound 3 (3.8×10^{-5} M) in the presence of 0.020 M CTAB after a direct pH jump from pH=1 to 3.48.
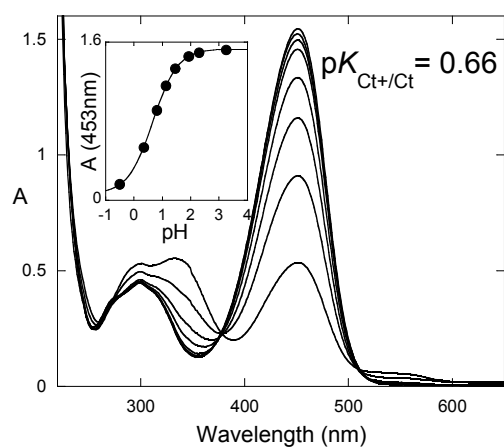
Figure S3C. Spectral variations of compound 3 (3.8x10^{-5} M) in the presence of 0.020 M CTAB micelles taken immediately after a reverse pH jump from equilibrated solutions of the *trans*-chalcone to acidic pH values.
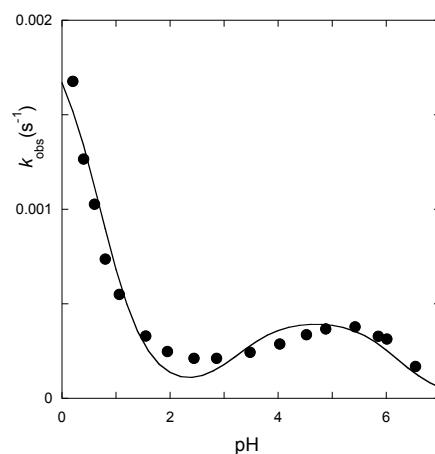

Figure S4C. Representation of the rate constants of compound 3 in the presence of 0.020 M CTAB for the slower process of the interconversion kinetics, versus pH. Fitting was achieved with eq.(11) for the following parameters: $K_h K_t k_i$=2.5x10^{-7} Ms^{-1}; $K_t k_i/k_{-h}$= 6.0x10^{-4} M; k_{-i}=1x10^{-5} s^{-1}; p$K_{Ct+/Ct}$=0.7; k_{-i+}=1.5x10^{-3} s^{-1}, k_h=4.2x10^{-4} s^{-1}.
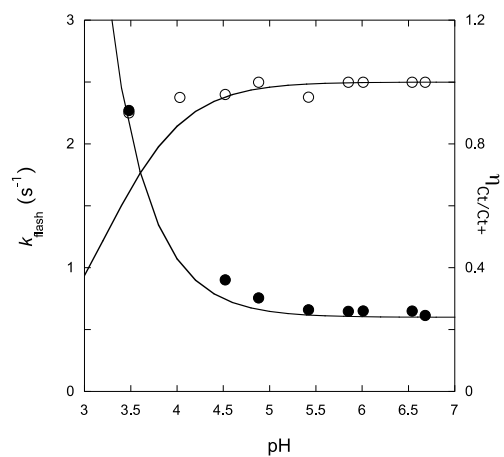
Figure S5C. Flash photolysis traces of the compound 3 in the presence of 0.020 M CTAB; fitting achieved with the data reported in the main text. Fitting was achieved with eq.(12) and eq.(13) for $K_t k_i/(1+K_t)=0.6$ and $k_{-h}/(1+K_t)= 1000$

---

[i] The change of regime, when tautomerization becomes slower than hydration occurs at very low pH values, but in these compounds this eff is masked by the superposition of the kinetic process resulting from protonation of the amines.